ACS OMEGA

http://pubs.acs.org/journal/acsodf

Article

Displacement Mechanisms of Residual Oil Film in 2D Microchannels

Jiawei Fan, Lili Liu,* Shanxin Ni, and Jing Zhao

Cite This: *ACS Omega* 2021, 6, 4155−4160

Read Online

ACCESS | Metrics & More | Article Recommendations

ABSTRACT: This paper explores displacement mechanisms of the residual oil film in microchannels by analyzing the following items after wetting hysteresis occurs: resistance on the residual oil film by the rock wall, the interfacial tension between displacement fluid and residual oil film, and horizontal stress acting on residual oil film by displacement fluids. Based on the continuity equations, motion equations, and constitutive equations of viscoelastic fluid, the numerical simulation is used to calculate the distribution of horizontal stress acting on the residual oil film by displacement fluids with different rheological properties. The results of the study show that increasing the horizontal stress on the oil film fundamentally mobilized the oil film and made it movable. Under the condition that the flow rate of the displacement fluid was constant, the value and direction of the horizontal stress acting on the oil film by the viscoelastic fluid changed. The elasticity changed the law of stress on the residual oil film, which is more conducive to mobilizing the oil film.

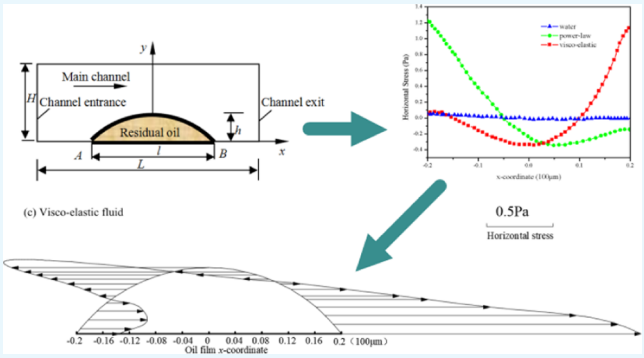

1. INTRODUCTION

A large amount of residual oil remains on the wall of the oil-wet rock after the water flooding, and how to mobilize it and make it movable is a key problem to be solved urgently. Therefore, many researchers have carried out a large number of experimental and theoretical studies. Wang et al.[1,2] studied the mechanism of how viscoelastic fluids improve oil displacement efficiency and proposed the concept of micro-forces. Liu et al.[3,4] treated "potential fields" as a research basis and the dynamic to displace oil by steam injection as a benchmark, introduced the concepts of "flow" and "force" of irreversible thermodynamics into the oil displacement process, and interpreted the mechanism of oil displacement by steam injection as three field synergies, i.e., the synergy between the dynamic potential fields, the synergy between the resistance potential fields, and the synergy between dynamic potential field and resistance potential field. Sun et al.[5] studied the oil displacement mechanism of continuous and dispersed phase flooding agents and found that SMG dispersion has better performance in increasing oil production and lowering water production. Bataweel et al.[6,7] conducted research on the oil displacement mechanism of cross-linked polymer using the computed tomography (CT) technique. Hellevang et al.[8−10] presented CO_2 enhanced oil recovery (EOR) mechanism in low-pressure, low-porosity, and low-permeability reservoirs. Seright et al.[11−14] conducted research on profile controlling and flooding performance, penetration performance, and oil displacement mechanism of polymer microspheres dispersion system in matrix-fracture medium and presented its micro-scopic profile controlling and flooding mechanism in a fractured low-permeability medium and stepwise deeper profile controlling and flooding mechanism in a fractured matrix. Kamal et al.[15−19] analyzed the oil displacement mechanism of alternate injection with polymer solutions with different viscoelasticities and concluded that alternately injecting polymer solutions with different viscoelasticities can alleviate the problem of excessive solution absorption in large channels and insufficient solution absorption in small channels, allowing more polymer solution with low molecular weight and low mass concentration to enter the low-permeability layer so that the flow rate of viscoelastic polymer solution in the high-permeability layer is further reduced and that in the low-permeability layer is further increased. Cense et al.[20−24] studied the seepage law of polymer flooding from both theoretical and experimental aspects.

This paper analyzes the displacement mechanism of the residual oil film from the perspective of stress on the residual oil film and compares the distribution laws of the displacement force on the residual oil film by displacement fluids with different rheological properties. It aims to lay the foundation

Received: September 22, 2020
Accepted: January 26, 2021
Published: February 5, 2021

https://dx.doi.org/10.1021/acsomega.0c04667
ACS Omega 2021, 6, 4155−4160

for the theoretical study of the deformation and mobilization of residual oil film under stress.

2. RESULTS AND DISCUSSION

2.1. Analysis of the Stress on the Oil Film. In this paper, it is suitable to use the upper-convected Maxwell (UCM) constitutive equation to describe the rheological properties of polymer solution in a reservoir because UCM belongs to a viscoelastic fluid model with its first normal stress difference as the main feature and the second normal stress difference equaling zero, and its constitutive equation contains only one relaxation time, which is relatively simple. The constitutive equation is as follows

$$\tau^{ik} + \lambda \overset{\nabla}{\tau}^{ik} = \eta_0 A^{ik} \tag{1}$$

where λ is the relaxation time, s; η_0 is the zero-shear viscosity, Pa·s; A is the first-order Rivlin−Ericksen deformation tensor; and $\overset{\nabla}{\tau}$ is the upper-convected derivative.

$$A^{ik} = \sqrt{g^{kk} g^{ii}} \frac{A_{ik}}{\sqrt{g_{kk} g_{ii}}} = A_{ik} = v_{i,j} + v_{j,i} = \frac{\partial v_i}{\partial x_j} + \frac{\partial v_j}{\partial x_i} \tag{2}$$

Specifically

$$\overset{\nabla}{\tau}^{ik} = \frac{\partial \tau^{ik}}{\partial t} + v^m \frac{\partial \tau^{ik}}{\partial x^m} - \tau^{mk} \frac{\partial v^i}{\partial x^m} - \tau^{im} \frac{\partial v^k}{\partial x^m} \tag{3}$$

There is a two-phase flow when polymer solution flows through residual oil. Residual oil belongs to the dispersed phase, while the polymer solution belongs to the continuous phase. They have different rheological properties. The polymer solution belongs to viscoelastic fluid, while the residual oil is a nonelastic non-Newtonian fluid (this paper assumes that the residual oil is a Newtonian fluid with constant density and viscosity).

When the oil film in contact with the rock wall surface is in a static state, regardless of the influence of gravity, the oil film is symmetrical with the same wetting angles, and the displacement fluid is stationary. This paper takes the oil film on the oil-wet rock as an example, and the stress is shown in two-dimensional Figure 1.

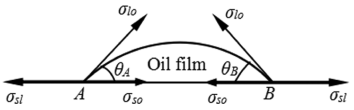

Figure 1. Stress on the oil film on the oil-wet rock surface.

In the equilibrium equation of interfacial tension at A and B points of the triphase contact on the surface of the oil-wet rock, i.e., Laplace equation, the oil film is symmetrical, and the wetting angle at A equals to that at B, i.e., $\theta_A = \theta_B = \theta$, which satisfies

$$\cos\theta = \frac{\sigma_{sl} - \sigma_{so}}{\sigma_{lo}} \tag{4}$$

where θ is the wetting angle, θ_A is the contact angle formed by the displacement of the oil film−rock contact by the displacement fluid−rock contact, i.e., the receding angle, θ_B is the contact angle formed by the displacement of the displacement fluid−rock contact by the oil film−rock contact, i.e., the advancing angle, σ_{sl} is the interfacial tension between the displacement fluid and the rock, σ_{so} is the interfacial tension between the oil film and the rock, and σ_{lo} is the interfacial tension between the displacement fluid and the oil film.

When the displacement fluid flows from left to right, the adhesion between the oil film and the oil-wet rock increases due to the adsorption, diffusion, and cementation between the oil film and the rock, and it becomes difficult to displace the entire oil film. The oil film deforms and wetting hysteresis occurs. The wetting angles at A and B change, resulting in $\theta_A < \theta_B$ (Figure 2). Due to the change in the wetting angles, the

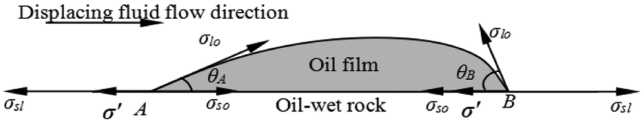

Figure 2. Stress on oil film after wetting hysteresis.

interfacial tension at A and B no longer satisfies the Laplace equation, and there must be a stress σ' to balance the stress on the oil film after the wetting hysteresis.[25,26] At this time, the equilibrium equations of the horizontal stress at A and B are

$$\sigma_{lo}\cos\theta_A - \sigma_{sl} + \sigma_{so} - \sigma' = 0 \tag{5}$$

$$-\sigma_{lo}\cos\theta_B - \sigma_{so} + \sigma_{sl} - \sigma' = 0 \tag{6}$$

Figure 2 shows $\theta_A < \theta < \theta_B$. The σ' is the resistance to oil film migration and is generated by the force between the molecules, such as van der Waals force and electrostatic charge force.[27−30] As the displacement force becomes larger, σ' becomes increasingly larger and balances the wetting hysteresis. The force f_m that impedes the oil film migration due to the presence of σ' can be expressed as

$$f_m = \int_l \sigma' \, dl \tag{7}$$

The degree of oil film deformation depends on the displacement force and the interfacial tension σ_{lo} between the displacement fluid and the oil film. Under the assumption that the interfacial tension is isotropic, the force f_σ that impedes the deformation of the oil film due to the presence of the interfacial tension can be expressed as

$$f_\sigma = \int_s \sigma_{lo} \, ds \tag{8}$$

When the displacement fluid acts on the oil film to deform it, the interfacial tension impedes the deformation of the oil film, causing the oil film to have a new shape.[31,32]

In summary, it is the resultant force of f_m and f_σ that impedes the overall movement of the oil film. Only when the displacement force is greater than the resultant force of f_m and f_σ can the entire oil film move. The displacement force acting on the oil film is mainly the flow direction component of a resultant force of the normal force and the tangential force acting on the oil film by the displacement fluid. The stress state p at any point in the flow field can be solved by the continuity equation, the motion equation, and the constitutive equation used to describe the displacement fluid.[33,34] The flow direction of the displacement fluid is assumed to be the x-direction, and the displacement force F_x along the x-direction at any point on the contact between the displacement fluid and the oil film is

https://dx.doi.org/10.1021/acsomega.0c04667
ACS Omega 2021, 6, 4155−4160

$$F_x = \int_s p_x \, ds = \int_s (n_x p_{xx} + n_y p_{yx} + n_z p_{zx}) ds \quad (9)$$

where n_x, n_y, and n_z are the cosine of the angle between the normal to the displacement fluid−oil film contact and the x-, y-, and z-directions, respectively, p_x is the stress of the displacement fluid at any point on the oil film surface with the x-direction as the normal direction, and p_{xx}, p_{yx}, and p_{zx} are the x-direction components of the stress at any point on the oil film surface with the normal at the x-, y-, and z-direction, respectively.

The oil film deforms under the action of the displacement force, while the interfacial tension between the displacement fluid and the oil film prevents the oil film from deforming, and the contact angle between the oil film and the rock changes accordingly. If the displacement force on the oil film is greater than the resistance, i.e.,

$$F_x > f_\sigma + f_m \quad (10)$$

The entire oil film will migrate. Therefore, only by increasing the displacement forces acting on the oil film can the oil film be fundamentally mobilized into movable oil, so as to achieve the ultimate goal of displacement.

2.2. Calculation of the Horizontal Stress on Residual Oil Film. When the oil film is displaced by fluids with different rheological properties, the distribution of horizontal stress acting on the oil film differs.[35,36] Due to the complexity of the pore space, this paper carries out the numerical calculation of a simplified flow field. The simplified two-dimensional calculation area is shown in Figure 3, with the flow channel length L = 100 μm, the flow channel width w = 20 μm, the oil film length l = 40 μm, and the oil film height h = 10 μm.

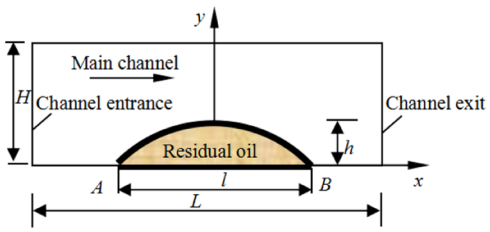

Figure 3. Two-dimensional calculation area of a simplified flow field.

In the later stage of oilfield development, water flooding is mainly used to enhance oil recovery. With the further exploitation of oil in the reservoir by water flooding, the surface stress of oil and rock in fracture increases gradually. As a Newtonian fluid, water is difficult to enhance oil recovery greatly. Therefore, this paper uses power-law fluid and viscoelastic fluid as a displacement fluid to achieve the purpose of enhancing oil recovery. In the numerical calculation of the simplified flow field, the physical parameters of displacement fluid are shown in Table 1.

Boundary conditions are set: inlet flow and outlet flow are equal and volume flow is 2×10^{-10} m^3/s; oil film is assumed to be Newtonian fluid and its viscosity is 20 mPa·s.

The curve of horizontal stress acting on the oil film by displacement fluids with different rheological properties is shown in Figure 4, where the positive value indicates that the horizontal stress direction is the same as the x-direction, and the negative value indicates that the horizontal stress direction is opposite to the x-direction.

Table 1. Physical Parameters of Displacement Fluid

displacement fluid	physical parameters
water	viscosity 1 mPa·s, density 1000 kg/m^3
power-law fluid	consistency coefficient 30 mPa·s, rheological index 0.8
viscoelastic fluid	zero-shear viscosity 30 mPa·s, relaxation time 0.6 s, density 1100 kg/m^3 (the upper-convected Maxwell constitutive equation is used to describe the characteristics of viscoelastic fluid)

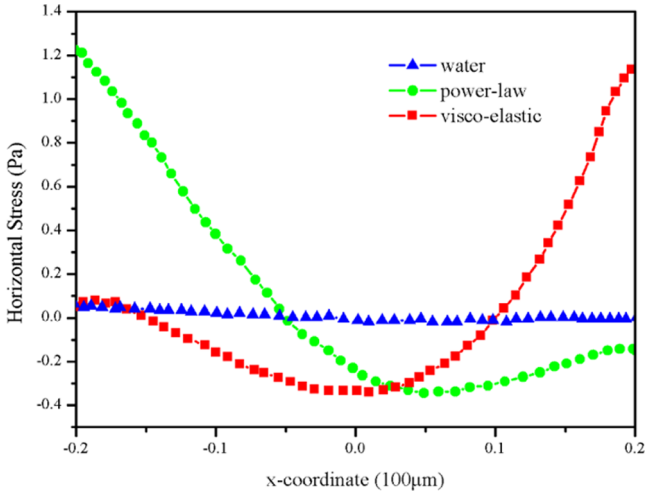

Figure 4. Horizontal stress acting on the oil film by displacement fluids with different rheological properties.

It can be seen from Figure 4 that water is a Newtonian fluid with relatively low viscosity, and the horizontal stress acting on the oil film is relatively small. The upstream oil film is subjected to positive horizontal stress, while the downstream oil film is subjected to negative horizontal stress; the positive horizontal stress and the negative one are distributed symmetrically with respect to the center of the oil film. As for the power-law fluid with a consistency coefficient of 30 mPa·s, the horizontal stress acting on the oil film is greater, and the upstream oil film is subjected to positive horizontal stress, but the horizontal stress on the oil film is 0 at the x-coordinate of −5 μm and turns slightly negative at the x-coordinate from −5 to 20 μm. As for the viscoelastic fluid with a relaxation time of 0.6 s, the horizontal stress acting on the oil film is completely different from that of water and power-law fluid. At the x-coordinate from −15 to 10 μm, the horizontal stress on the oil film is negative, but that at other locations is positive and big. It is the elasticity of the viscoelastic fluid that changes the law of stress on the residual oil film, making the oil film more prone to overall migration. To clarify the value and direction of the horizontal stress acting on the oil film by the aforementioned three fluids, a vector diagram (Figure 5) is drawn.

It can be clearly seen from Figure 5 that the horizontal stresses of the viscoelastic fluid acting on the residual oil film near the rock wall are along the positive x-axis, i.e., horizontally to the right. The sum of the horizontal stresses to the right is beneficial to the overall mobilization and migration of the residual oil film, and the horizontal stresses to the left in the upper half of the oil film are more likely to cause local deformation of the residual oil film. When the displacement fluid is water and power-law fluid, the horizontal stresses in the

https://dx.doi.org/10.1021/acsomega.0c04667
ACS Omega 2021, 6, 4155−4160

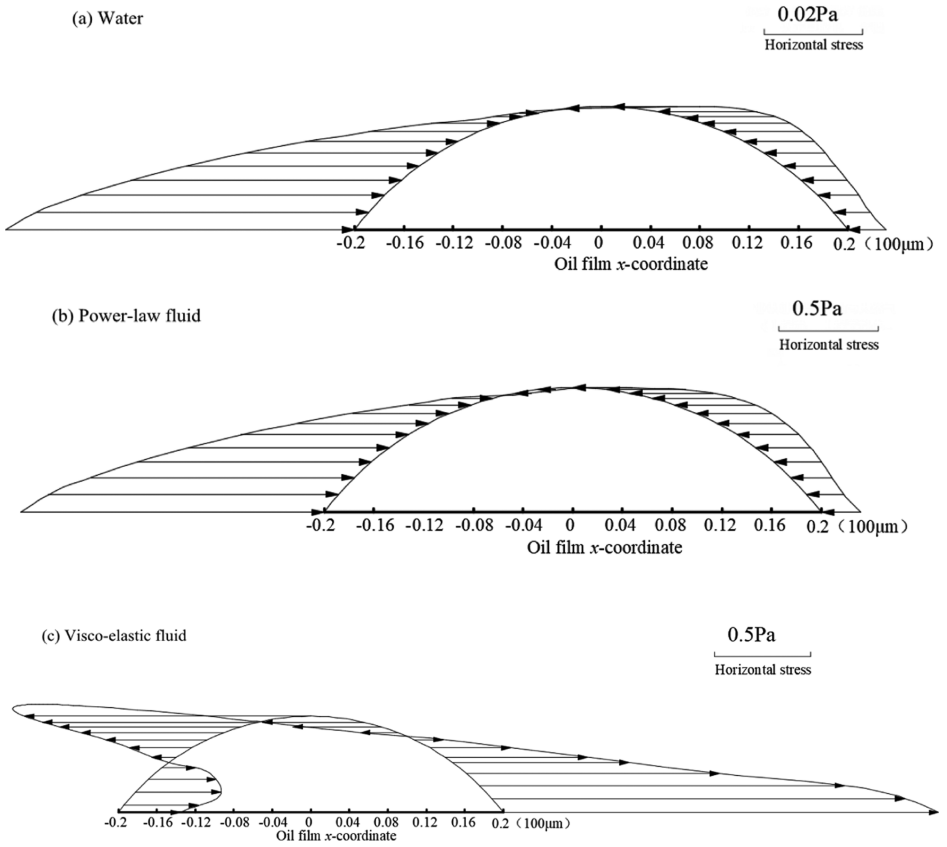

Figure 5. Vector diagram of horizontal stress acting on the oil film by displacement fluids with different rheological properties. (a) Calculation results of water. (b) Calculation results of power-law fluid. (c) Calculation results of viscoelastic fluid.

upstream and downstream are in opposite directions, so the sum of the horizontal stresses is greatly reduced, resulting in the small deformation of the residual oil film and difficulty in mobilizing the entire oil film.

There are 4256 grid nodes in the flow channel and 814 grid nodes in the remaining oil area. The number of unstructured grid nodes is much more than that of quadrilateral grid nodes. Taking the normal stress as an example, under the condition of the same $we = 0.2$ and the viscosity ratio $\lambda = 1$, the comparison of normal stress change curves of different grids is shown in Figure 6.

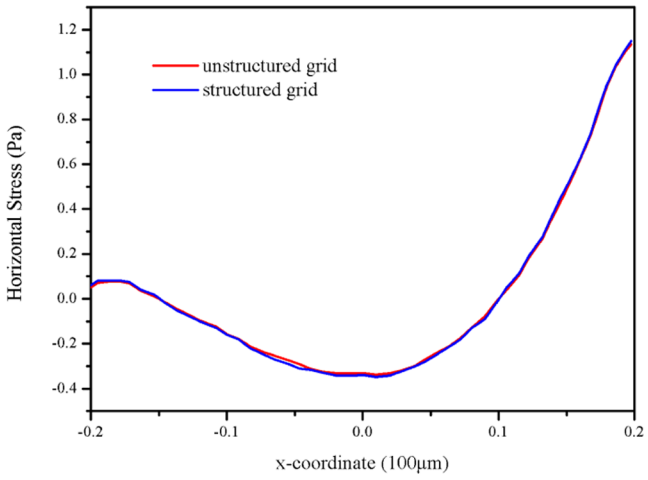

Figure 6. Horizontal stress changes with different meshing.

It can be seen from Figure 6 that under the same calculation conditions, whether an unstructured grid or quadrilateral grid is used in the calculation area, the variation curve of normal stress is basically the same and overlapped. Therefore, it is feasible to use a quadrilateral mesh.

When the pressure gradient, channel width, and oil film height are certain, water, power-law fluid, and viscoelastic fluid were used to drive oil, respectively. The oil film deformation on the rock surface with different wettabilities (Figure 7) shows that the deformation degree of the residual oil film on the rock surface increases significantly as the viscoelasticity of the replacement fluid increases. Initially, the wetting angles of oil films on the oil-wet rock, water-wet rock, and intermediate wet rock are 67.38, 90, and 126.87°, respectively. After oil film deformation, the deformation degree is described by the advancing angle and the receding angle. Compared with the case of water flooding, the advancing angle increases by 37.2% and the receding angle decreases by 74.7% when the residual oil film on the oil-wet rock surface was driven by viscoelastic fluid, as shown in Table 2. With viscoelastic fluid as the replacement fluid, the oil film on the oil-wet rock has a larger advancing angle and a smaller receding angle, and the oil film on the water-wet rock has the smallest advancing angle and the largest receding angle. In other words, when viscoelastic fluid with the same mass concentration is used to drive residual oil film on the rock with different wettabilities, the oil film deformation on the oil-wet rock surface is slightly larger than that on the intermediate wet rock surface, and the oil film deformation on intermediate wet rock surface is slightly larger than that on the water-wet rock. That is to say, the oil film on the oil-wet rock surface is easier to be stripped.

https://dx.doi.org/10.1021/acsomega.0c04667
ACS Omega 2021, 6, 4155−4160

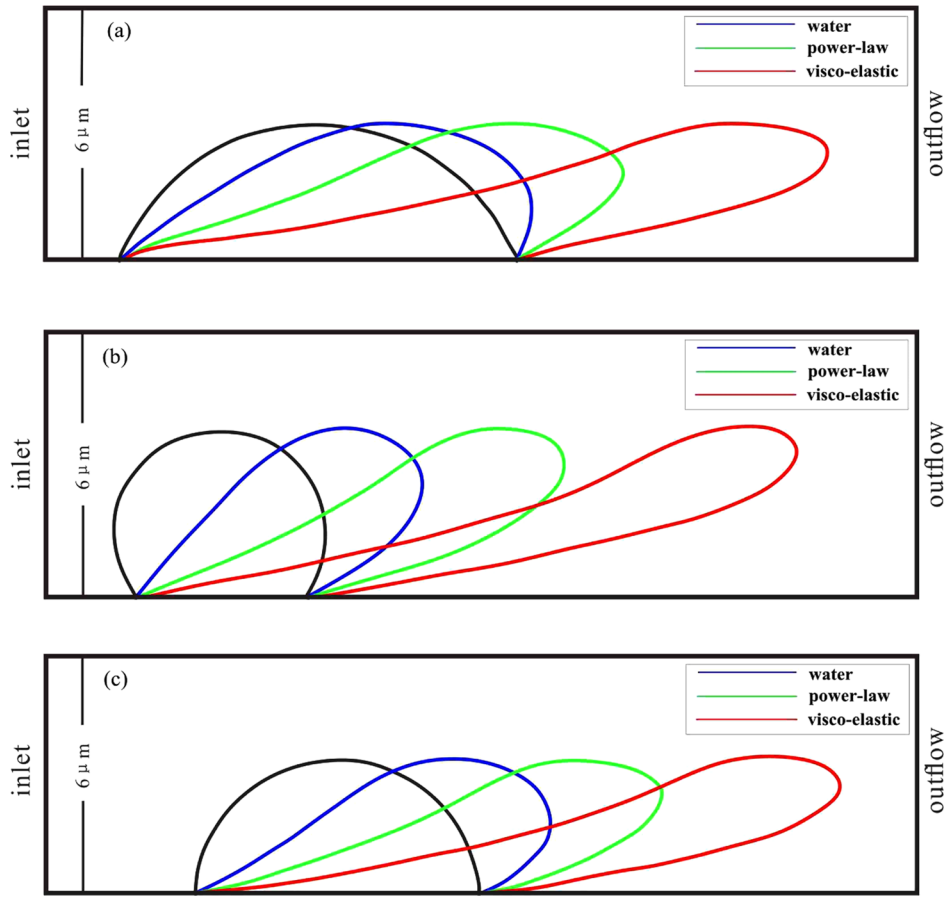

Figure 7. Deformation comparison of oil film on a rock surface with different wettabilities: ((a) oil-wet rock; (b) water-wet rock; and (c) intermediate wet rock).

Table 2. Comparison of Wetting Angle after Oil Film Deformation

	oil-wet rock		water-wet rock		intermediate wet rock	
displacement fluid	advancing angle (deg)	receding angle (deg)	advancing angle (deg)	receding angle (deg)	advancing angle (deg)	receding angle (deg)
water	124.23	31.53	154.14	53.79	147.22	30.88
power-law	165.24	15.54	158.38	21.65	162.96	15.83
viscoelastic	170.39	7.97	168.91	10.35	170.19	8.89

3. CONCLUSIONS

(1) What impedes the overall migration of oil film is the resultant force of f_m and f_σ. Only when the displacement force is greater than such a resultant force can oil film be mobilized and wholly migrate.

(2) The horizontal stress acting on the residual oil film by a viscoelastic fluid is different from that acting by water or power-law fluid. It is the elasticity of viscoelastic fluid that changes the law of stress on the residual oil film: the horizontal stress produced by viscoelastic fluid has a greater carrying effect on the oil film than the shear stress of Newtonian fluid acting on the oil film, which makes the partial migration of oil film happen.

(3) Higher viscoelasticity of the polymer solution leads to greater force on the residual oil film and more obvious asymmetry of the oil film, which makes the oil film more prone to deformation and bursting and causes the separation of small oil drops from the main body.

(4) The deformation degree of oil film differs for rocks with different wettabilities: the oil film on the surface of the oil-wet rock is more deformed than that on the surface of the water-wet rock.

AUTHOR INFORMATION

Corresponding Author

Lili Liu − *Department of Petroleum Engineering, Northeast Petroleum University, Daqing 163318, China*; Email: dqliull2009@163.com

Authors

Jiawei Fan − *Department of Petroleum Engineering, Northeast Petroleum University, Daqing 163318, China*; orcid.org/0000-0002-4254-9101

Shanxin Ni − *Tianjin Petroleum Vocational and Technical College, Tianjin 301600, China*

Jing Zhao − *Tianjin Petroleum Vocational and Technical College, Tianjin 301600, China*

Complete contact information is available at: https://pubs.acs.org/10.1021/acsomega.0c04667

https://dx.doi.org/10.1021/acsomega.0c04667
ACS Omega 2021, 6, 4155−4160

Notes

The authors declare no competing financial interest.

■ ACKNOWLEDGMENTS

This paper is financially supported by the University Nursing Program for Young Scholars with Creative Talents in Heilongjiang Province (grant no. UNPYSCT2016121) and the Northeast Petroleum University Youth Science Fund (grant no. 20182018QNL-45).

■ REFERENCES

(1) Wang, D. M.; Xia, H. F.; Yang, S. R.; Wang, G. The Influence of Visco-elasticity on Micro Forces and Displacement Efficiency in Pores, Cores and in the Field, *Soc. Pet. Eng.* **2010**, DOI: 10.2118/127453-MS.

(2) Wang, D. M.; Wang, G.; Wu, W. X.; Xia, H. F.; Yin, H. J. Influence of the Micro-force Produced by Viscoelastic Displacement Liquid on Displacement Efficiency. *J. Xi'an Shiyou Univ. (Nat. Sci. Ed.)* **2008**, *23*, 43−45.

(3) Liu, Y.; Fan, J. W.; Liu, L. L.; Yang, S. R. Numerical Simulation of Residual Oil Flooded by Polymer Solution in Microchannels. *Geofluids* **2018**, *2018*, 1−10.

(4) Fan, J. W.; Liu, Y.; Liu, L. L.; Yang, S. R. Hydrodynamics of residual oil droplet displaced by polymer solution in micro-channels of lipophilic rocks. *Int. J. Heat Technol.* **2017**, *35*, 611−618.

(5) Sun, Z.; Wu, X. C.; Kang, X. D.; Lu, X. G.; Li, Q.; Jiang, W. D.; Zhang, J. Comparison of oil displacement mechanisms and performances between continuous and dispersed phase flooding agents. *Pet. Explor. Dev.* **2019**, *46*, 121−129.

(6) Bataweel, M. A.; Nasr-El-Din, H. A.; Schechter, D. S. Fluid Flow Characterization of Chemical EOR Flooding: A Computerized Tomography (CT) Scan Study. *Soc. Pet. Eng.* **2011**, No. 943.

(7) Saraf, A.; De Zwart, A. H.; Currie Peter, K.; Ali Mohammad, A. Analysis of the Effect of Residual Oil on Particle Trapping During Produced-Water Reinjection Using X-Ray Tomography. *SPE J.* **2010**, *15*, 949−957.

(8) Wei, B.; Zhang, X.; Liu, J.; Xu, X. G.; Pu, W. F.; Bai, M. X. Adsorptive behaviors of supercritical CO_2 in tight porous media and triggered chemical reactions with rock minerals during CO_2-EOR and -sequestration. *Chem. Eng. J.* **2020**, *381*, No. 122577.

(9) Hellevang, H.; Pham, V. T. H.; Aagaard, P. Kinetic modelling of CO_2 −water−rock interactions. *Int. J. Greenhouse Gas Control* **2013**, *15*, 3−15.

(10) Pham, V. T. H.; Lu, P.; Aagaard, P.; Zhu, C.; Hellevang, H. On the potential of CO_2−water−rock interactions for CO_2 storage using a modified kinetic model. *Int. J. Greenhouse Gas Control* **2011**, *5*, 1002−1015.

(11) Han, H. Y. Study on Flow Mechanism of Polymer Microspheres Dispersion System in Fractured Low Permeability Reservoir. Beijing University of Science and Technology Press: Beijing, 2018; pp 48−57.

(12) Seright, R. S. How much polymer should be injected during apolymer flood? Review of previous and current practices. *SPE J.* **2017**, *22*, 1−18.

(13) Xia, H.; Wang, D.; Wu, W.; Jiang, H. Effect of the viscoelasticity of displacing fluids on the relationship of capillary number and displacement efficiency in weak oil-wet cores. *Soc. Pet. Eng* **2008**, No. 109228.

(14) Jiang, H.; Wu, W.; Wang, D.; Zeng, Y.; Zhao, S.; Nie, J. The effect of elasticity on displacement efficiency in the lab and results of high concentration polymer flooding in the field proceedings. *Soc. Pet. Eng.* **2008**, No. 137610110.

(15) Sun, C.; Guo, H.; Li, Y.; Song, K. Recent Advances of Surfactant-Polymer (SP) Flooding Enhanced Oil Recovery Field Tests in China. *Geofluids* **2020**, *2020*, 1−16.

(16) Kamal, M. S.; Sultan, A. S.; Al-Mubaiyedh, U. A.; Hussein, I. A. Review on Polymer Flooding: Rheology, Adsorption, Stability, and Field Applications of Various Polymer Systems. *Polym. Rev.* **2015**, *55*, 491−530.

(17) You, Q.; Wang, K.; Tang, Y. C.; Zhao, G.; Liu, Y. F.; Zhao, M. W.; Li, Y. Y.; Dai, C. L. Study of a Novel Self-Thickening Polymer for Improved Oil Recovery. *Ind. Eng. Chem. Res.* **2015**, *54*, 9667−9674.

(18) Zhang, P.; Wang, Y.; Yang, Y.; Zhang, J.; Cao, X.; Song, X. The effect of microstructure on performance of associative polymer: In solution and porous media. *J. Pet. Sci. Eng.* **2012**, *90*−*91*, 12−17.

(19) Kamal, M. S.; Sultan, A. S.; Al-Mubaiyedh, U. A.; Hussein, I. A. Review on polymer flooding: rheology, adsorption, stability, and field applications of various polymer systems. *Polym. Rev.* **2015**, *55*, 491−530.

(20) Cense, A.; Berg, S.; Bakker, K.; Jansen, E. Direct Visualization of Designer Water Flooding in Model Experiments. *Soc. Pet. Eng.* **2011**, No. 108822541.

(21) Huh, C.; Pope, G. A. Residual Oil Saturation from Polymer Floods: Laboratory Measurements and Theoretical Interpretation. *Soc. Pet. Eng.* **2008**, No. 96078260.

(22) Wever, D. A. Z.; Picchioni, F.; Broekhuis, A. A. Polymers for Enhanced Oil Recovery: A Paradigm for Structure-Property Relationship in Aqueous Solution. *Prog. Polym. Sci.* **2011**, *36*, 1558−1628.

(23) Pivello, M. R.; Villar, M. M.; Serfaty, R.; Roma, A. M.; Silveira-Neto, A. A fully adaptive front tracking method for the simulation of two phase flows. *Int. J. Multiphase Flow* **2014**, *58*, 72−82.

(24) Izbassarov, D.; Muradoglu, M. A front-tracking method for computational modeling of viscoelastic two-phase flow systems. *J. Non-Newtonian Fluid Mech.* **2015**, *223*, 122−140.

(25) Wang, X. D.; Peng, X. F.; Min, J. C. Hysteresis of Contact Angle at Liquid-solid Interface. *J. Eng. Thermophys.* **2002**, *23*, 67−70.

(26) Wang, X. D.; Peng, X. F.; Li, D. Z. Stress singularity of dynamic contact Angle and contact line. *Sci. China* **2003**, *33*, 625−631.

(27) Splet Peter, D. M. Shear Flow Past Two-Dimensional Droplets Pinned or Moving on an Adhering Channel Wall at Moderate Reynolds Numbers: a Numerical Study. *J. Fluid Mech.* **2006**, *561*, 439−463.

(28) Chung, C.; Lee, M.; Char, K.; Ahn, K. H.; Lee, S. J. Droplet dynamics passing through obstructions in confined microchannel flow. *Microfluid. Nanofluid.* **2010**, *9*, 1151−1163.

(29) Luz, A.-B.; Taehun, L. Single bubble rising dynamics for moderate Reynolds number using Lattice Boltzmann Method. *Comput. Fluids* **2010**, *39*, 1191−1207.

(30) Bhardwaj, S.; Dalal, A.; Biswas, G.; Mukherjee, P. P. Analysis of droplet dynamics in a partially obstructed confinement in a three-dimensional channel. *Phys. Fluids* **2018**, *30*, No. 102102.

(31) Yokoi, K. A Numerical Method for Free-Surface Flows and Its Application to Droplet Impact on a Thin Liquid Layer. *J. Sci. Comput.* **2008**, *35*, 372−396.

(32) Leshansky, A. M.; Pismen, L. M. Breakup of drops in a microfluidic T junction. *Phys. Fluids* **2009**, *21*, No. 023303.

(33) Liu, L. L.; Yang, S. R.; Fan, J. W. Stress Calculation of Polymer Displacing Residual Oil in Micro Pores. *Int. J. Performability Eng.* **2017**, *13*, 211−220.

(34) Navarro, R.; Zinchenko, A. Z.; Davis, R. H. Boundary-integral study of a freely suspended drop in a T-shaped microchannel. *Int. J. Multiphase Flow* **2020**, *130*, No. 103379.

(35) Wang, F.; He, F. A Numerical Method for Two_Phase Flow in Micro Channels and Its Application to Droplet Control by Electrowetting on Dielectric. *Acta Phys. Sin.* **2006**, *55*, 1005−1010.

(36) Ceniceros, H. D.; Nós, R. L.; Roma, A. M. Three-dimensional, fully adaptive simulations of phase-field fluid models. *J. Comput. Phys.* **2010**, *229*, 6135−6155.

https://dx.doi.org/10.1021/acsomega.0c04667
ACS Omega 2021, 6, 4155−4160